

High-Temperature Setup for X-Ray Absorption Spectroscopy at the ASTRA Beamline of the SOLARIS Centre

K. GADOMSKI^a, Ł.S. PUCHAŁA^b, M. MALINOWSKA^{a,c}, A. PUCHALSKI^a,
K.J. GRZYWA^b, J. TURCZYŃSKI^d, G. GAZDOWICZ^e, A. MAXIMENKO^e,
N.K.C. MUNIRAJU^f, T.K. PIETRZAK^a AND W. TABIŚ^{b,*}

^aWarsaw University of Technology, Faculty of Physics, Koszykowa 75, 00-662 Warsaw, Poland

^bAGH University of Krakow, Faculty of Physics and Applied Computer Science, al. A. Mickiewicza 30, 30-059 Krakow, Poland

^cInstitute of High Pressure Physics of the Polish Academy of Sciences, Sokółowska 29/37, 01-142 Warsaw, Poland

^dInstitute of Physics of the Polish Academy of Sciences (IFPAN), al. Lotników 32/46, 02-668 Warsaw, Poland

^eSOLARIS National Synchrotron Radiation Centre, Jagiellonian University, Czerwone Maki 98, 30-392 Krakow, Poland

^fThe Henryk Niewodniczanski Institute of Nuclear Physics, Polish Academy of Sciences, Radzikowskiego 152, 31-342 Krakow, Poland

Received: 30.12.2025 & Accepted: 08.04.2026

Doi: [10.12693/APhysPolA.149.S211](https://doi.org/10.12693/APhysPolA.149.S211)

*e-mail: wtabis@agh.edu.pl

Synchrotron radiation facilities offer intense and tunable X-ray beams, enabling time-efficient acquisition of X-ray absorption spectra, such as X-ray absorption near-edge structure and extended X-ray absorption fine structure, with temporal resolution comparable to the characteristic timescales of structural transformations, including crystallization processes in glasses. In this work, we present the design and implementation of a high-temperature sample holder developed for the ASTRA beamline at the SOLARIS Synchrotron in Kraków, Poland. The holder supports *in situ* and *operando* X-ray absorption spectroscopy experiments in both transmission and fluorescence detection modes at temperatures up to 500°C. Its performance was validated through temperature-dependent X-ray absorption spectroscopy measurements of binary vanadate–phosphate glasses undergoing crystallization. The preliminary results confirm the stability, reliability, and applicability of the setup for tracking thermally induced structural changes in solid-state materials using absorption spectroscopy.

topics: XANES/EXAFS, *in situ* measurements, high temperature, vanadate glasses

1. Introduction

Synchrotron light sources have become essential tools in modern science, providing intense, highly collimated, and tunable X-ray beams that enable advanced structural and spectroscopic investigations across disciplines, including materials science, chemistry, energy storage, catalysis, and environmental science. The SOLARIS Centre, located in Kraków, Poland, is a third-generation light source operating at 1.5 GeV and designed to support a diverse range of analytical techniques [1, 2], one of which is X-ray absorption spectroscopy (XAS).

XAS is a powerful element-specific technique that probes the local atomic and electronic structure of materials. It is based on measuring the absorption coefficient of a material as a function of incident photon energy across a selected absorption edge. In general, XAS can be divided into two regimes, i.e., X-ray absorption near-edge structure (XANES or NEXAFS) and extended X-ray absorption fine structure (EXAFS). XANES focuses on the region within approximately 50 eV of the absorption edge and provides information on the oxidation state, coordination geometry, and unoccupied electronic states of the absorber atom. This region is sensitive to multiple-scattering processes and to electronic

transitions (e.g., $1s \rightarrow 3d$ pre-edge transitions and dipole-allowed $1s \rightarrow 4p$ transitions at the main edge in $3d$ transition metals), making it highly useful for chemical analysis. EXAFS, on the other hand, covers the higher-energy region (typically 50–1000 eV above the edge), where the oscillations in absorption arise from interference between the outgoing photoelectron wave and those scattered by neighboring atoms. EXAFS analysis yields quantitative information on interatomic distances, coordination numbers, and structural disorder.

Among several SOLARIS beamlines dedicated to XAS, ASTRA (Absorption Spectroscopy beamline for Tender energy Range and Above) offers capabilities tailored for XAS measurements in transmission and fluorescence detection modes, under ambient as well as *in situ/operando* conditions, covering a photon energy range of 1–15 keV, with an emphasis on the 1.8–12 keV region. This energy range provides access to the K -edges of elements such as Si, P, and S, as well as the K -edges of $3d$ transition metals (such as Ti, V, Cr, Mn, Fe, Co, Ni, Cu, and Zn) and L -edges of heavier elements, making ASTRA particularly suitable for research in catalysis, energy materials, coordination chemistry, and environmental sciences. The beamline delivers a photon flux on the order of 10^9 – 10^{10} ph s⁻¹ eV⁻¹ with a beam size up to of 10×1 mm², ensuring excellent signal-to-noise conditions.

Building upon its current capabilities and energy coverage, the ASTRA beamline provides an excellent platform for the development of customized experimental probes aimed at enabling *in situ* and *operando* XAS experiments at elevated temperatures. The high photon flux, broad energy range, and compatibility with various gas environments make it ideal for studying thermally activated processes, including crystallization, phase transitions, redox reactions, and structural rearrangements in functional materials.

In this work, we focus on extending ASTRA’s capabilities by developing a dedicated sample holder system that allows for heating samples from room temperature up to 500°C while maintaining compatibility with both transmission and fluorescence detection geometries. This technical advancement supports the growing demand for *operando* measurements of materials under conditions that closely mimic their real-world application environments, such as in catalysis, battery cycling, and glass structure evolution.

To validate the functionality of the newly developed high-temperature sample holder, we present a preliminary *in situ* XANES/EXAFS study of the nanocrystallization process in $95\text{V}_2\text{O}_5 \cdot 5\text{P}_2\text{O}_5$ glasses — a model system chosen for its well-documented structural complexity and relevance in electrochemical and optical applications. These glasses offer an ideal test platform due to their relatively simple binary composition, moderate glass transition and crystallization temperatures

(compatible with the holder’s operational range up to 500°C), and their extensive prior characterization using techniques such as differential scanning calorimetry (DSC) and X-ray diffraction (XRD) [3, 4]. Notably, the thermally induced nanocrystallization process in vanadate-phosphate glasses leads to a significant enhancement in electronic conductivity [5] — an effect of both scientific and technological appeal. Despite the high interest, the evolution of the local atomic structure during crystallization, particularly in the early stages of nanocrystallite formation, has not yet been probed using X-ray absorption spectroscopy.

The newly implemented high-temperature setup at the ASTRA beamline addresses this gap by enabling XANES/EXAFS measurements under controlled thermal conditions at elevated temperatures. The initial results confirm the stability and performance of the holder and demonstrate ASTRA’s growing potential as a platform for *operando* XAS studies of solids. This development represents a significant advancement in extending ASTRA’s capabilities beyond ambient conditions, paving the way for systematic investigations of temperature-driven local structural transformations in glasses, nanomaterials, and amorphous systems.

2. High-temperature sample holder

2.1. Design

The custom-built high-temperature sample holder, shown in Fig. 1, was developed to enable *in situ* and *operando* XAS measurements in two modes:

- (i) transmission — where the absorption coefficient is determined from the ratio of incident and transmitted intensities measured with ionization chambers;
- (ii) fluorescence — where the emitted fluorescence photons can be detected by an energy-dispersive detector placed near the sample, at 90° to the incident beam.

The main body of the holder was machined from copper due to its high thermal conductivity, which facilitates efficient and uniform heat distribution around the sample. The support rod was constructed from ceramic to provide thermal insulation and electrical isolation from the chamber environment.

The copper block contains two channels: one for a cylindrical cartridge heater and the other for a thermocouple, as shown in Fig. 1a. This arrangement ensures effective thermal coupling between the heating element and the sample region while also allowing for accurate temperature monitoring near the sample. Detailed dimensions of the holder are provided in Fig. 1b. The fully assembled probe is

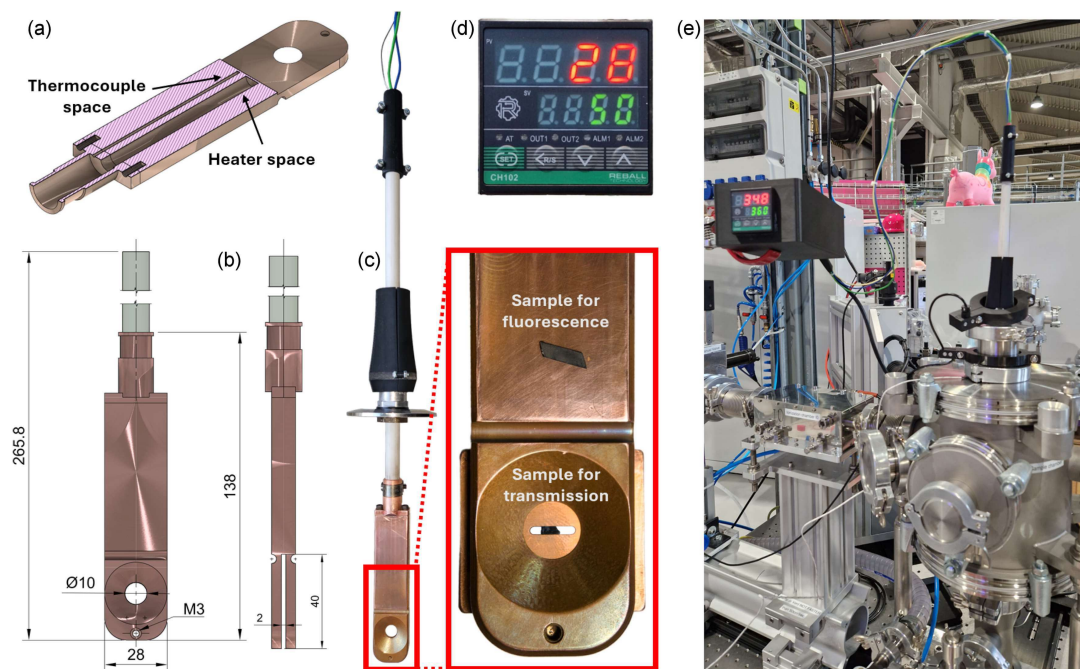


Fig. 1. High-temperature XAS setup developed for the ASTRA beamline at the SOLARIS Centre. (a) Cross-sectional view of the copper sample holder, highlighting the dedicated grooves for the cylindrical heater and thermocouple to ensure uniform and controlled heating of the sample area. (b) Schematic with key dimensions of the holder, including sample mount geometry and mounting interfaces. (c) Assembled sample holder mounted on a KF-50 vacuum flange, with ceramic insulation for thermal and electrical isolation. The inset shows designated positions for XAS measurements in transmission and fluorescence modes. (d) Temperature controller used to regulate the heater, displaying both the setpoint and actual process value from the thermocouple. (e) Operational view of the high-temperature holder integrated into the experimental chamber at the ASTRA beamline, illustrating its compatibility with the beamline infrastructure and control systems.

mounted on a KF-50 vacuum flange, with the heater and thermocouple wires enclosed in a ceramic tube to prevent mechanical and thermal damage during operation (Fig. 1c). An electrical feedthrough is connected through a standard port, and a custom gasket is used to maintain the exchange gas pressure.

Temperature regulation was carried out using a Reball Technology CH102 controller (Fig. 1d), which allows precise setting of the target temperature (SV) and displays the current sample temperature (PV) based on the feedback from the thermocouple. The setup provides reliable thermal stability up to 500°C under atmospheric or low-vacuum conditions and integrates smoothly with the experimental station at the ASTRA beamline (Fig. 1e).

To facilitate rapid sample exchange and minimize beamline downtime, samples were pre-mounted onto removable mini-holders, designed to fit precisely onto the main copper head. Each mini-holder carries the sample for transmission measurements and is mounted by a simple screw mechanism. This modular design allows samples to be prepared in advance and then quickly replaced during beamtime, significantly improving experimental efficiency for temperature-dependent XAS studies.

For measurements in fluorescence detection geometry, the sample can be attached directly to the copper holder using a conductive high-temperature silver epoxy. In the present setup, commercially available silver paste (e.g., DuPont 6838), stable up to approximately 600°C, can be used to ensure good thermal contact and mechanical stability during heating. To minimize parasitic signals originating from the copper holder, the vertical dimension of the sample must exceed the vertical size of the incident X-ray beam. At the ASTRA beamline, the typical beam dimensions are approximately 10 mm (horizontal) \times 1 mm (vertical). Therefore, the sample height in the vertical direction should be larger than 1 mm to ensure that the beam interacts only with the sample surface. The beam dimensions can also be adjusted using slits, allowing the horizontal beam size to be reduced from the maximum width of 10 mm if necessary.

2.2. Temperature calibration

Before conducting experiments at the ASTRA beamline, an off-line temperature calibration and safety validation protocol was carried out to ensure

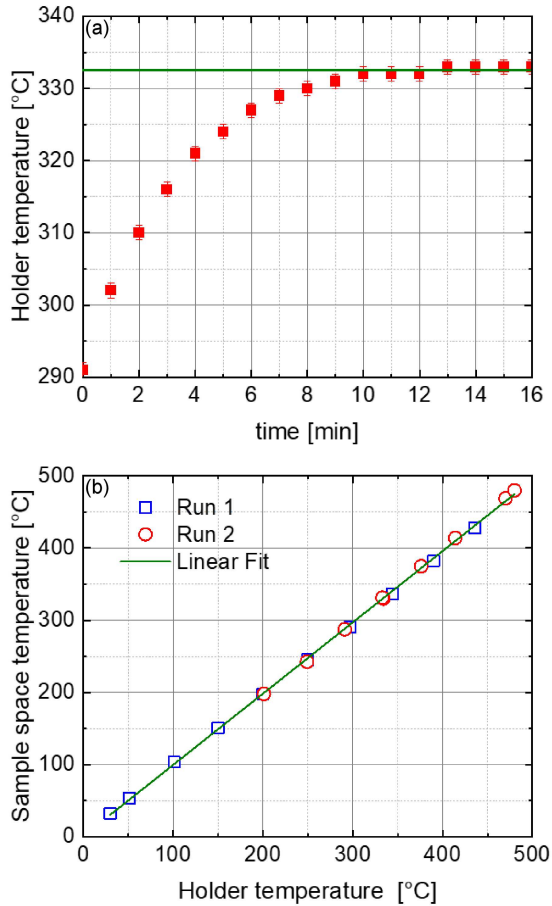


Fig. 2. Temperature calibration of the high-temperature sample holder. (a) Temperature evolution of the holder during a representative 50°C heating step, showing an exponential approach to thermal equilibrium. The green line indicates the stabilized target temperature, which was reached within ≈ 10 min. (b) Correlation between the temperature measured at the sample position (external thermocouple) and the internal thermocouple embedded in the holder. Data from two independent calibration runs are shown. The linear fit (green line) yields a slope of 0.997, demonstrating excellent agreement and confirming that the internal thermocouple accurately reflects the sample temperature across the entire tested range (from RT to 500°C).

the reliable and secure operation of the high-temperature sample holder at temperatures up to 500°C in a high-purity argon and nitrogen atmosphere. The primary objective was to verify that the system could safely reach and maintain the target temperatures without exceeding material limitations or compromising experimental integrity. The secondary goal was to determine the temperature stabilization time after each heating step. A third objective was to assess the actual temperature in the sample region, near the transmission sample position, and compare it with the internal thermocouple readings used during standard operation.

During the tests, an additional K-type thermocouple was temporarily installed in proximity to the transmission sample position, while the internal thermocouple embedded in the holder remained in its dedicated channel. The holder was heated incrementally in controlled steps, and temperature readings of both thermocouples were recorded. The thermal stabilization profile was monitored throughout the process to evaluate heating dynamics and response time. The temperature response during a representative 50°C heating step is shown in Fig. 2a. The temperature exhibited an exponential increase with time, which is characteristic of resistive heating systems with thermal inertia. The time required to reach thermal stability was ≈ 10 min. Comparable stabilization times were observed throughout the entire operational range from room temperature (RT) to 500°C.

The system exhibited stable thermal behavior throughout the tested temperature range, with the temperature measured at the sample location closely following the values recorded by the internal thermocouple embedded in the holder. Figure 2b presents the temperature measured by the external thermocouple placed near the sample as a function of the internal thermocouple temperature. Data points from two independent heating runs overlap consistently, confirming excellent reproducibility. A linear fit to the data yields a slope of 0.997, indicating a nearly one-to-one correspondence between the sample temperature and the internal thermocouple reading. These results validate that, under the tested conditions, the internal thermocouple provides an accurate representation of the actual sample temperature, with negligible systematic deviation.

3. Test absorption measurements

3.1. Synthesis and preliminary sample characterization

The vanadate–phosphate glass material with nominal composition $95\text{V}_2\text{O}_5 \cdot 5\text{P}_2\text{O}_5$ was prepared using a standard melt quenching technique. Appropriate amounts of reagents, i.e., V_2O_5 (Sigma-Aldrich, 99.5%) and $(\text{NH}_4)\text{H}_2\text{PO}_4$ (POCH — Polish Chemicals, 99.5%), were ground and mixed in a mortar. A platinum crucible with the batch was placed in a Czylok PRC 100x150/180/OTS furnace preheated to 900°C, and the melt was held for 15 min in an air atmosphere. The molten mixtures were rapidly poured onto a copper plate held at room temperature and immediately covered by another identical plate. As a result, it was possible to synthesize glassy parallel-plate samples with a thickness of slightly less than 100 μm .

X-ray diffraction (XRD) measurements were performed to ensure the full amorphousness of the synthesized glass. For this purpose, a Malvern

Panalytical Empyrean diffractometer was used in the Bragg–Brentano configuration, equipped with a copper tube.

3.2. Sample preparation for XAS measurements

For optimal transmission-mode XAS measurements at the vanadium *K*-edge (5465 eV), the ideal thickness of the $95\text{V}_2\text{O}_5 \cdot 5\text{P}_2\text{O}_5$ glass sample was estimated. Assuming a mass absorption coefficient of approximately $200 \text{ cm}^2/\text{g}$ and a bulk density of 3.4 g/cm^3 , the resulting linear absorption coefficient is $\mu \approx 680 \text{ cm}^{-1}$. To achieve a total absorption of $\mu d \approx 2.5$, the optimal sample thickness is $d \approx 37 \text{ }\mu\text{m}$.

Due to limitations in the melt-casting synthesis process, binary vanadate-phosphate glass samples could not be reliably fabricated with a thickness below $70\text{--}80 \text{ }\mu\text{m}$. To obtain thinner specimens suitable for transmission-mode XAS at the vanadium *K*-edge, samples were mechanically thinned using a manual polishing procedure. Each sample was mounted onto a polishing chuck using high-temperature-resistant wax (Fig. 3a). Sequential polishing was performed with silicon carbide abrasive papers of decreasing grit size to gradually reduce the thickness. The thickness of the sample was periodically verified using an optical microscope equipped with a digital camera and measurement software with a calibrated length scale. The thickness was determined from side-view images of the sample edge, such as the one presented in Fig. 3b. During the polishing process, the sample was inspected frequently, particularly when approaching the target thickness range, in order to avoid over-polishing. This procedure allowed controlled thinning of the samples to a final thickness of $\approx 30\text{--}50 \text{ }\mu\text{m}$.

Once the target thickness was achieved, the polished samples were mounted on the copper holder (Fig. 3c) using DuPont 6838 silver epoxy to ensure good thermal contact and mechanical stability. A matching copper cover plate with an elliptical beam window (Fig. 3d) was then placed over the sample to define the beam path and further improve thermal anchoring. The assembly, consisting of the holder, the thinned glass sample, and the cover, was then inserted into the high-temperature sample probe for XAS measurements, as described in Fig. 1c.

3.3. X-ray absorption spectroscopy

The preliminary XAS test measurements were performed at the vanadium *K*-edge in transmission mode. Both the ionization chambers and the sample chamber were purged with nitrogen gas maintained at a pressure of 250 Torr to minimize absorption

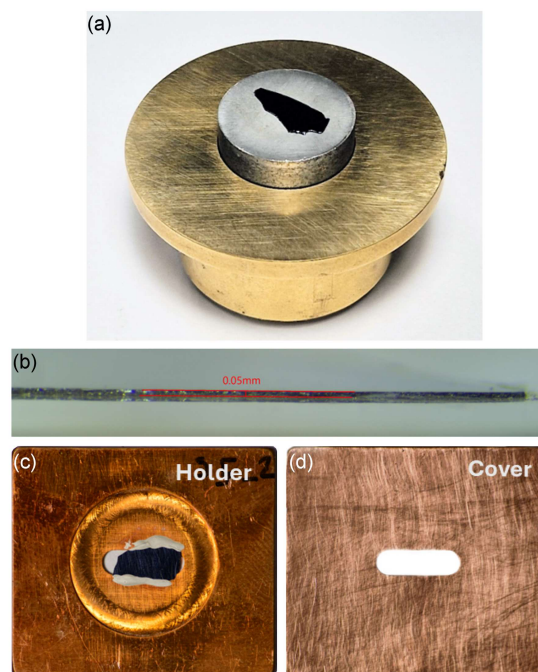


Fig. 3. Sample preparation procedure. (a) Manual polishing fixture with the binary-oxide glass sample mounted on the cylindrical support using wax. Samples with an initial thickness of $\sim 300 \text{ }\mu\text{m}$ were mechanically polished to a final thickness of $30\text{--}50 \text{ }\mu\text{m}$. (b) Optical microscope side-view image of a polished sample used to determine the sample thickness. The thickness was measured from calibrated microscope images using dedicated analysis software. (c) The polished sample mounted in the copper holder and secured with DuPont 6838 silver epoxy. (d) Copper cover plate used during measurements. The oval slit in both the holder and the cover defines the beam path and ensures proper thermal anchoring of the sample during the experiment. The sample, sandwiched between the holder and the cover, is then installed in the measurement assembly, as shown in Fig. 1c.

by atmospheric components. A Ge(220) double-crystal monochromator was employed to monochromatize the polychromatic synchrotron beam from the bending magnet source. The energy was calibrated by aligning the first derivative maximum of a vanadium metal foil to 5465 eV, ensuring accurate energy referencing across all spectra.

The incident beam was shaped using precision slits to produce a rectangular spot with dimensions of approximately 5 mm (width) $\times 1 \text{ mm}$ (height). XAS spectra were collected over an energy range from 5300 to 6250 eV, covering the pre-edge, near-edge (XANES), and extended (EXAFS) regions. The acquisition time was fixed at 1 s per energy point. A variable energy step size was used. Namely, fine steps of 0.25 eV were applied near the edge region to capture detailed electronic structure features, while larger steps were used in the pre-edge

and post-edge regions to optimize acquisition time, i.e., up to 10 eV in the pre-edge region and up to 2 eV in the EXAFS region. Each complete spectrum required ≈ 30 min of measurement time. To ensure reproducibility and improve the signal-to-noise ratio, two spectra were recorded at each temperature. Post-processing of the data, including normalization, background subtraction, and extraction of EXAFS oscillations, as well as Fourier transform analysis for radial distribution function calculations, was performed using the *Demeter* software package [6].

To evaluate the performance of the developed high-temperature sample holder and to demonstrate its suitability for *operando* XAS investigations, a series of temperature-dependent X-ray absorption experiments was conducted. Measurements were designed to cover the relevant thermal regime of the material, beginning below the glass transition temperature and extending beyond the crystallization range. The binary V_2O_5 - P_2O_5 glasses with a high content of V_2O_5 are known to undergo crystallization around 240–250°C [4]. Accordingly, XAS spectra were acquired at room temperature and subsequently at temperatures ranging from 160 to 440°C in 20°C increments. This temperature protocol enabled the monitoring of local structural evolution during the thermally induced glass-to-crystal transition.

4. XAS results

Two representative XAS spectra collected during the temperature-dependent measurements are presented in Fig. 4. Panel (a) shows the normalized absorption spectra for the initial glass and the sample measured at 400°C, with the XANES region in the inset. Panel (b) shows the magnitude of the Fourier transform of the EXAFS signal, corresponding to the radial distribution function (RDF). The inset in panel (b) presents the corresponding k^2 -weighted EXAFS oscillations $\chi(k)$, illustrating clear changes in amplitude and oscillation pattern after thermal treatment. The first spectrum, recorded at room temperature, corresponds to the initial amorphous glassy state of the sample. The second spectrum was acquired at 400°C, after the sample had undergone partial crystallization.

Comparison of the vanadium K -edge XANES spectra of the pristine and annealed at 400°C glasses (inset in Fig. 4a) shows that the pre-edge feature retains nearly the same energy (shift of only about 0.3 eV to higher energy after annealing) and exhibits only a slight increase in intensity, indicating that the average oxidation state of vanadium and the local site symmetry remain essentially unchanged upon annealing [7, 8]. In contrast, the main absorption edge of the as-quenched glass is shifted by about 1.0 eV to higher energy relative

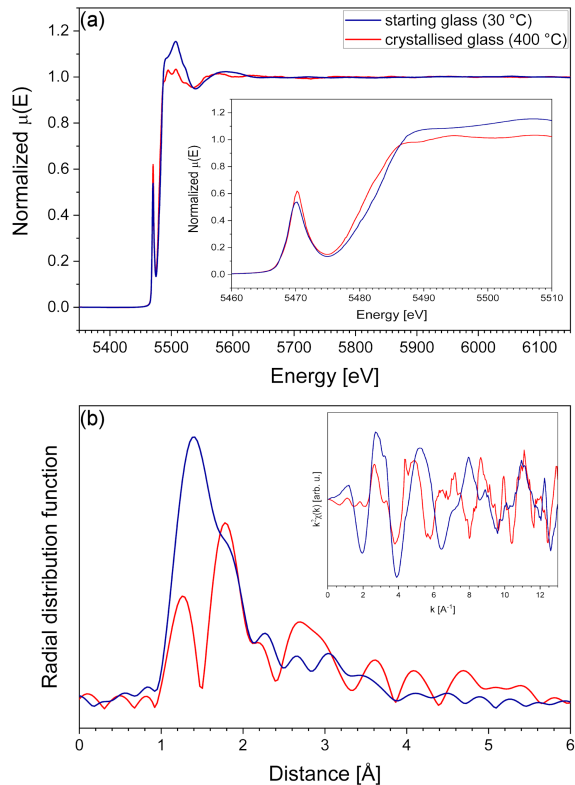


Fig. 4. Comparison of X-ray absorption spectra of the V_2O_5 - P_2O_5 glass measured at room temperature (30°C) and after thermal treatment at 400°C. (a) Normalized V K -edge XANES spectra. The inset shows the near-edge region in detail. (b) The magnitude of the Fourier-transformed EXAFS signal representing the radial distribution function (RDF). Distinct changes in the V–O and V–V coordination shells are observed after crystallization. The inset shows k^2 -weighted EXAFS oscillations $\chi(k)$, highlighting differences in the local atomic environment after annealing.

to the annealed sample, suggesting a subtle modification of the V–O bonding and local electronic structure — such as changes in covalency or network connectivity — rather than a significant redox transformation of vanadium. These differences reflect alterations in the local atomic structure around vanadium atoms and are consistent with a transition from a disordered glassy matrix to a more ordered (nano)crystalline phase.

Substantial modifications are observed for corresponding radial distribution functions (RDFs), derived from the Fourier transforms of the EXAFS oscillations and shown in Fig. 4b. For the glassy sample, a single well-defined peak appears at ≈ 1.4 Å, corresponding to the first coordination shell (V–O bonds). After crystallization at elevated temperature, the first shell splits into two distinct peaks at ≈ 1.25 Å and 1.8 Å, indicating the emergence of two different V–O bond lengths, characteristic of a more ordered local structure. Additionally,

a second-shell feature centered at around 2.7 Å becomes apparent, corresponding to V–V interactions, further confirming the onset of crystallization and medium-range ordering. These differences reflect alterations in the local atomic structure around vanadium atoms and are consistent with a transition from a disordered glassy matrix to a more ordered (nano)crystalline phase.

While a full analysis of the entire temperature series will provide more detailed information on the kinetics and structural pathways of the crystallization process in V₂O₅–P₂O₅ glasses, such an investigation is beyond the scope of this publication. The current study focuses on validating the performance of the newly developed high-temperature sample holder for temperature-resolved XAS experiments. A comprehensive analysis of the crystallization mechanism and structural evolution will be presented in a forthcoming publication.

5. Conclusions

This work presents the design, implementation, and validation of a high-temperature sample holder developed for the ASTRA beamline at the SOLARIS National Synchrotron Radiation Centre, enabling X-ray absorption spectroscopy (XANES/EXAFS) measurements under controlled thermal conditions. The holder supports both transmission and fluorescence detection geometries and is compatible with beamline operation in temperature range up to 500°C in controlled gas atmospheres. While transmission mode offers improved spectral quality, the studied samples must be thin, typically below 100 μm, requiring dedicated sample preparation protocols, which were successfully developed and demonstrated for V₂O₅–P₂O₅ glasses.

Preliminary experiments confirmed the thermal stability and accuracy of the setup, as well as its capability to capture structural transformations associated with thermally induced crystallization. The acquired XANES and EXAFS data exhibit high signal-to-noise ratios and enable investigation of changes in local atomic coordination, validating the applicability of the system for *in situ* and *operando* studies.

Acknowledgments

This publication was partially developed under the provision of the Polish Ministry of Science and Higher Education project “Support for research and development with the use of research infrastructure of the National Synchrotron Radiation Centre SOLARIS” under contract no. 1/SOL/2021/2. We acknowledge the SOLARIS Centre for access

to the ASTRA beamline, where the measurements were performed. Further development of the ASTRA beamline at NSRC SOLARIS was supported within the EU Horizon 2020 program (952148-Sylinda). K.G., M.M., A.P., and T.K.P. are grateful to the National Science Centre (NCN), Poland, for support in the framework of a grant OPUS-23 no. 2022/45/B/ST5/04005. The work at the AGH University was supported by the National Science Centre, Poland, grant OPUS (grant no. UMO2021/41/B/ST3/03454) and a subsidy of the Ministry of Science and Higher Education of Poland.

References

- [1] J. Hormes, W. Klysubun, J. Göttfert et al., *Nucl. Instrum. Methods Phys. Res. B* **489**, 76 (2021).
- [2] J. Szlachetko, J. Szade, E. Beyer et al., *Eur. Phys. J. Plus* **138**, 10 (2023).
- [3] T. Pietrzak, J. Garbarczyk, I. Gorzkowska, M. Wasiucionek, J. Nowinski, S. Gierlotka, P. Jozwiak, *J. Power Sources* **194**, 73 (2009).
- [4] T.K. Pietrzak, M. Wasiucionek, J.L. Nowiński, J.E. Garbarczyk, *Solid State Ion.* **251**, 78 (2013).
- [5] T.K. Pietrzak, M. Wasiucionek, J.E. Garbarczyk, *Nanomaterials* **11**, 1321 (2021).
- [6] B. Ravel, M. Newville, *J. Synchrotron Radiat.* **12**, 537 (2005).
- [7] P. Chaurand, J. Rose, V. Briois, M. Salome, O. Proux, V. Nassif, L. Olivi, J. Susini, J.-L. Hazemann, J.-Y. Bottero, *J. Phys. Chem. B* **111**, 5101 (2007).
- [8] X. Lu, L. Deng, S.A. Saslow et al., *J. Phys. Chem. B* **125**, 12365 (2021).